Supporting Information

Spontaneous and Induced Chiral Symmetry Breaking of Stereolabile Pillar[5]arene Derivatives upon Crystallisation

Haiying Wang,[a] Weiwei Yang,[a] Kim K. Baldridge,[a] Caihong Zhan,*[b] Tushar Ulhas Thikekar,*[a,c] Andrew C.-H. Sue*[c]

a. School of Pharmaceutical Science & Technology, Tianjin University, 92 Weijin Road, Nankai District, Tianjin 300072, P. R. China.
b. College of Chemistry and Life Sciences, Zhejiang Normal University, 688 Yingbin Road, Jinhua, Zhejiang Province 321004, P. R. China.
c. College of Chemistry and Chemical Engineering, Xiamen University, 422 Siming S Rd, Siming District, Xiamen, Fujian Province 361005, P. R. China.

* Corresponding E-mail address: andrewsue@xmu.edu.cn; tusthikekar@tju.edu.cn; chzhan@zjnu.cn

Table of Contents

1. Materials and General Methods

Starting materials, reagents, and solvents were purchased from commercial vendors and used as received, unless otherwise noted. Analytical thin-layer chromatography (TLC) was performed on aluminum sheets, precoated with silica gel GF_{254}. Flash column chromatography was performed over silica gel (200−300 mesh). ^{1}H, ^{13}C NMR spectra were recorded on a Bruker Advance 400 MHz spectrometers at room temperature, unless otherwise noted. The electronic circular dichroism (ECD) spectra were recorded on a MOS-500 spectrophotometer. Solid state samples were prepared using the KBr pellet technique (e.g. 40 mg of KBr per 0.5 mg sample, finely ground), then mounted on a pellet sample holder for ECD analysis. The ECD spectra were recorded in the range 800 to 190 nm, a step size of 1 nm, a bandwidth of 4 nm, a step of 1 s, and an acquisition period of 0.05 s.

2. Synthetic Procedures

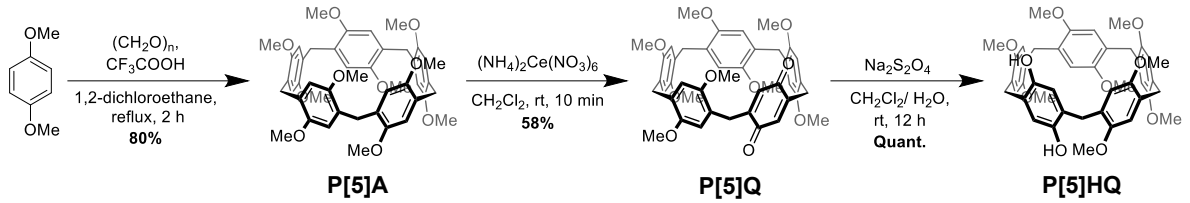

Scheme S1: The synthetic route of *rac*-**P[5]A**, *rac*-**P[5]Q**, and *rac*-**P[5]HQ**. Only one chiral conformation of each pillar[5]arene derivative is shown.

rac-**P[5]A** (DMP[5]): To a solution of 1,4-dimethoxybenzene (2.77 g, 20 mmol) and paraformaldehyde (0.60 g, 20 mmol) in 1,2-dichloroethane (200 mL), trifluoroacetic acid (10 mL) was added. The reaction mixture was refluxed for 2 h. After cooling, the reaction mixture was poured into methanol. The resulting precipitate was collected by filtration. Another fraction was obtained after filtrate evaporation and precipitation with methanol. The crude product was subjected to column chromatography ($CHCl_3$/EtOAc = 100:0 to 99:1, *v*/*v*) to afford **P[5]A** (2.40 g, 80%). The NMR data is in accordance with literature.[1]

rac-**P[5]Q** (pillar[4]arene[1]quinone): To a solution of **P[5]A** (1.5 g, 2 mmol) in CH_2Cl_2 (100 mL), an aqueous solution of $(NH_4)_2Ce(NO_3)_6$ (2.2 g, 4 mmol) was added. The resulting red-coloured mixture was stirred at room temperature for 10 min, washed with water (100 mL × 3), and concentrated under reduced pressure. The residue was subjected to chromatography (EtOAc/*n*-hexane＝1∶9, *v*/*v*) to afford **P[5]Q** product as a red solid (812 mg, 58%). The NMR data is in accordance with literature.[2]

rac-**P[5]HQ** (pillar[4]arene[1]hydroquinone): A solution of **P[5]Q** (500 mg, 0.70 mmol) in CH_2Cl_2 (30 mL) was stirred in a 50 mL round–bottom flask while an aqueous solution of $Na_2S_2O_4$ (2.40 g, 13.9 mmol) was added. The mixture was stirred at room temperature for 12 h. The water layer was extracted by CH_2Cl_2 (50 mL × 3). The combined organic phase was washed with water (100 mL), brine (100 mL), and dried over anhydrous Na_2SO_4. After the solvent was filtered and removed under reduced pressure, **P[5]HQ** was obtained as a white solid quantitatively. The NMR data is in accordance with literature.[2]

3. Resolution by Triage

Saturated solution of **P[5]HQ** was prepared and degassed by bubbling Ar gas for 10 min. The sample was placed in a sealed 20 mL vial containing ethyl ether, and left to stand at room temperature. Single crystals grown by vapor-liquid diffusion were collected by using tweezers and sorted with the aid of a Leica DM2000 microscope with a DFC295 camera.

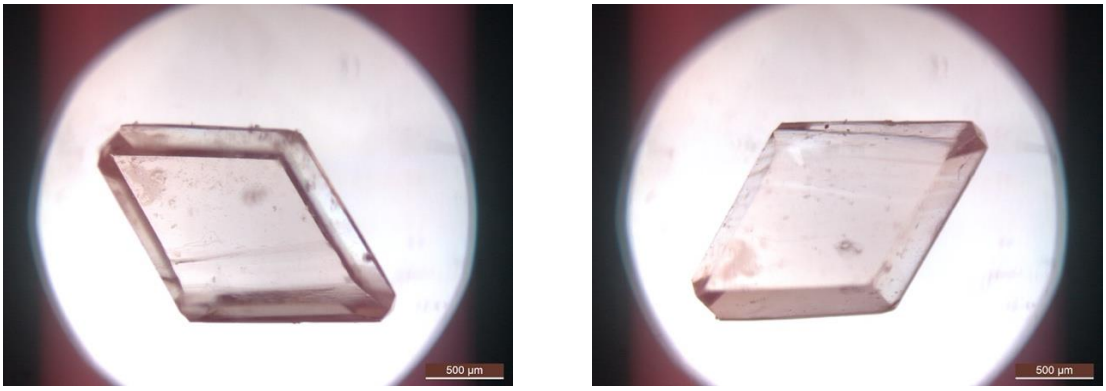

Fig. S1 Original optical microscope images of a **P[5]HQ** single crystals obtained. Both sides of the same crystal were photographed.

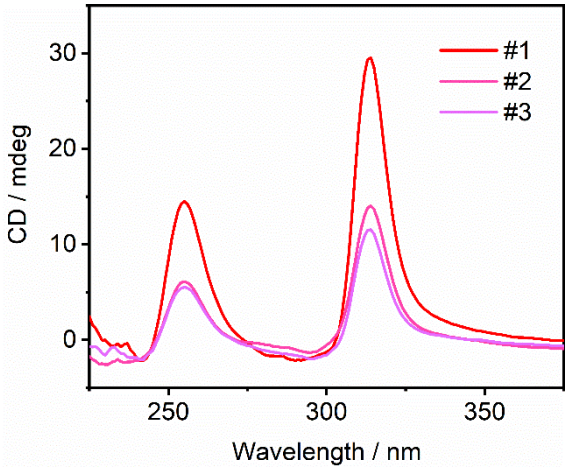

Fig. S2 Solid-state ECD spectra of three different handpicked (*M*)-**P[5]HQ** single crystals

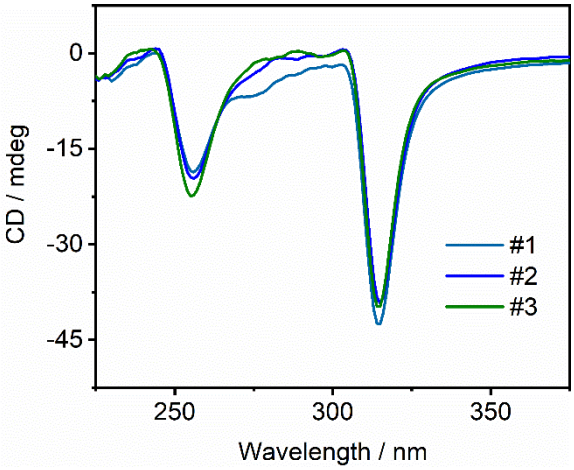

Fig. S3 Solid-state ECD spectra of three different handpicked (*P*)-**P[5]HQ** single crystals.

4. Computational Details for Simulated ECD Spectra

Full geometry optimisations were performed and uniquely characterised via second derivatives (Hessian) analysis to establish stationary points. The B97-D[3] density functional method with an ultrafine grid was used in combination with the Def2-TZVPP basis set.[4] Absorption energies were computed in CH_2Cl_2 (DCM) at the TD-B97xD[5]/Def2-TZVPP(DCM)//B97-D/Def2-TZVPP(DCM) level of theory. From the TD-DFT results, ECD spectra were simulated also in DCM solvent using a Gaussian band shape assumption.[6] Effects of solvent in all cases employed the COSMO:*ab initio* continuum method.[7,8] Visualization and analysis of structural and property results were obtained using Avogadro[9] and GaussView.[10]

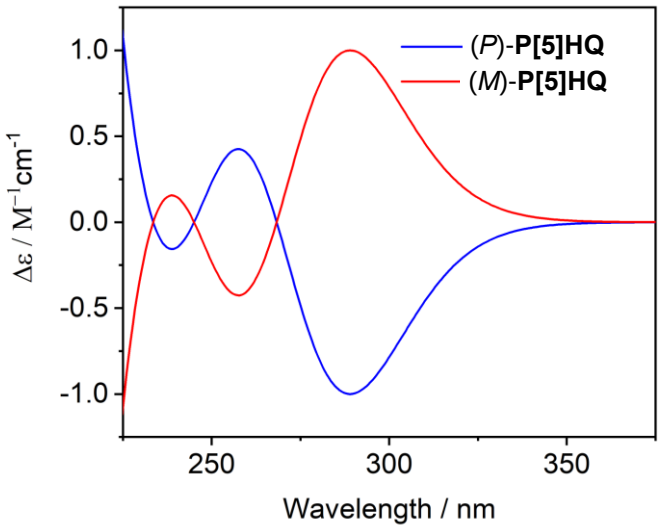

Fig. S4 Simulated ECD spectra of (*P*)/(*M*)-**P[5]HQ**.

5. Viedma's Ripening

Crystalline sample of *rac*-**P[5]HQ** was obtained by vapor diffusion method. A sample vial containing a near-saturated solution of **P[5]HQ** in CH_2Cl_2 was placed in a sealed container with ethyl ether inside, and left to stand at room temperature overnight. Crystalline powder of *rac*-**P[5]HQ** (0.15 g) and grinding media (2.0 g of 0.8 mm YTZ Zirconia ceramic beads) were suspended in a saturated solution of **P[5]HQ** in CH_2Cl_2 (1 mL) in a 10-mL sealed tube. The sample was then stirred by a magnetic stir bar (10 mm × 4 mm, oval shape) at 1400 rpm. The **P[5]HQ** slurry was sampled using syringe needle and deposited on filter paper to dry prior to ECD analysis. The sealed tube was replenished with the same volume of saturated **P[5]HQ** CH_2Cl_2 solution after each sampling.

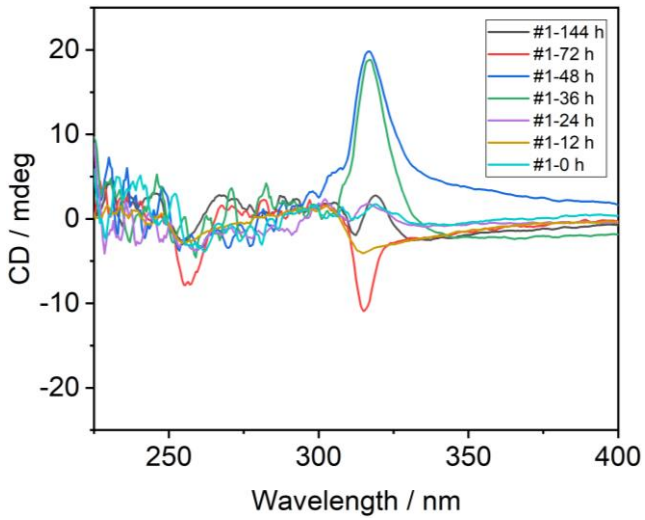

Fig. S5 Solid-state ECD spectra of a **P[5]HQ** sample showing reversal of signs of Cotton effect during the Viedma ripening process.

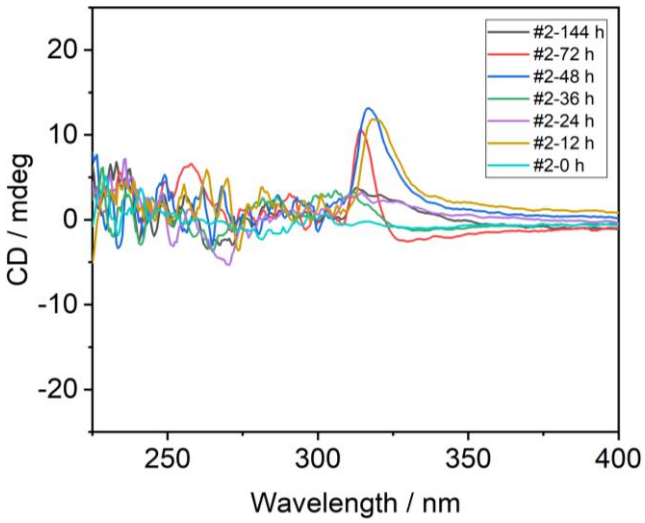

Fig. S6 Solid-state ECD spectra of a **P[5]HQ** sample showing on and off Cotton effect during the process of Viedma ripening.

6. Chiral Induction by Ethyl Lactate

- Direct crystallisation of *rac*-**P[5]HQ** in *D*/*L*-ethyl lactate

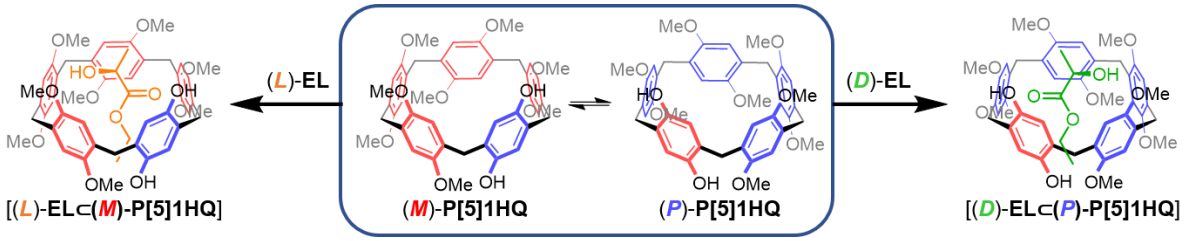

Scheme S2: The synthetic route of [(*L*)-**EL**⊂(*M*)-**P[5]HQ**] and [(*D*)-**EL**⊂(*P*)-**P[5]HQ**] inclusion complexes.

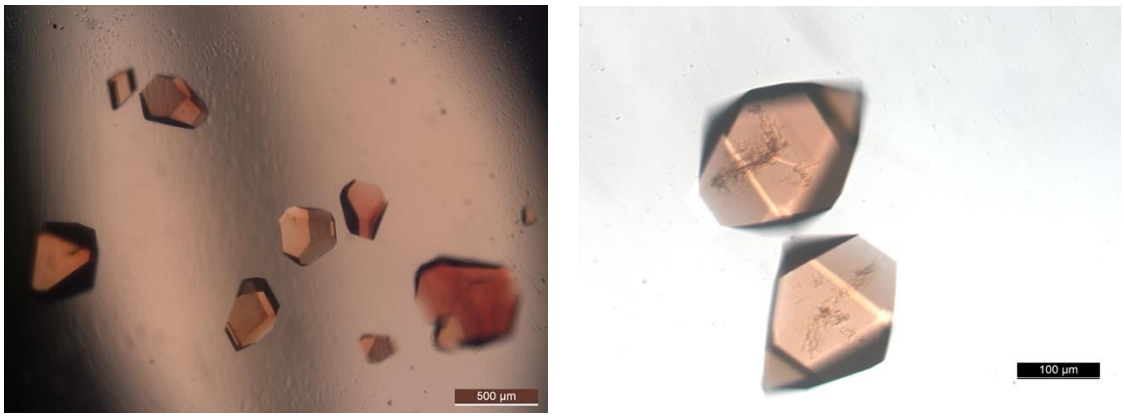

Fig. S7 Original optical microscope images of [(*L*)-**EL**⊂(*M*)-**P[5]HQ**] (left) and [(*D*)-**EL**⊂(*P*)-**P[5]HQ**] (right) single crystals.

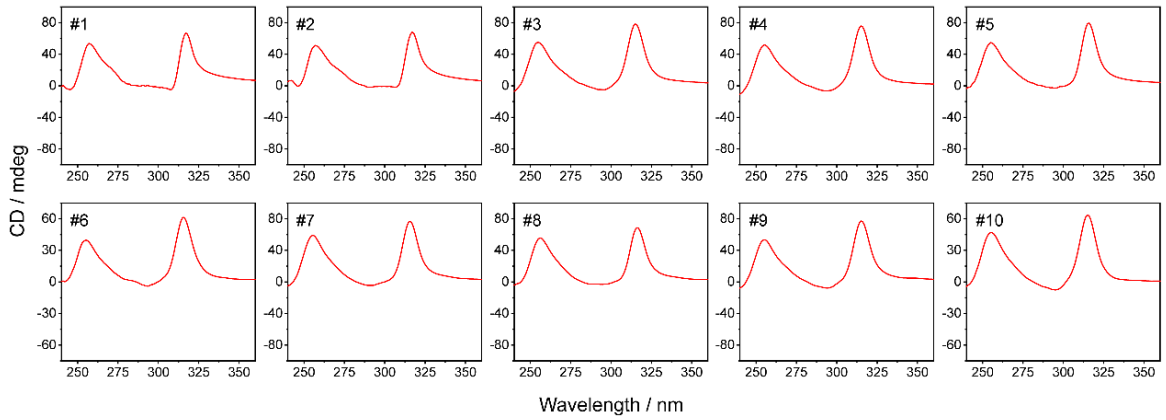

Fig. S8 Solid-state ECD spectra of 10 independent **P[5]HQ** samples crystallised in (*L*)-**EL**. Solid-phase samples were prepared using 50 mg KBr and 1 mg of crystalline powder. All 10 samples showed positive Cotton effects at 259/315 nm.

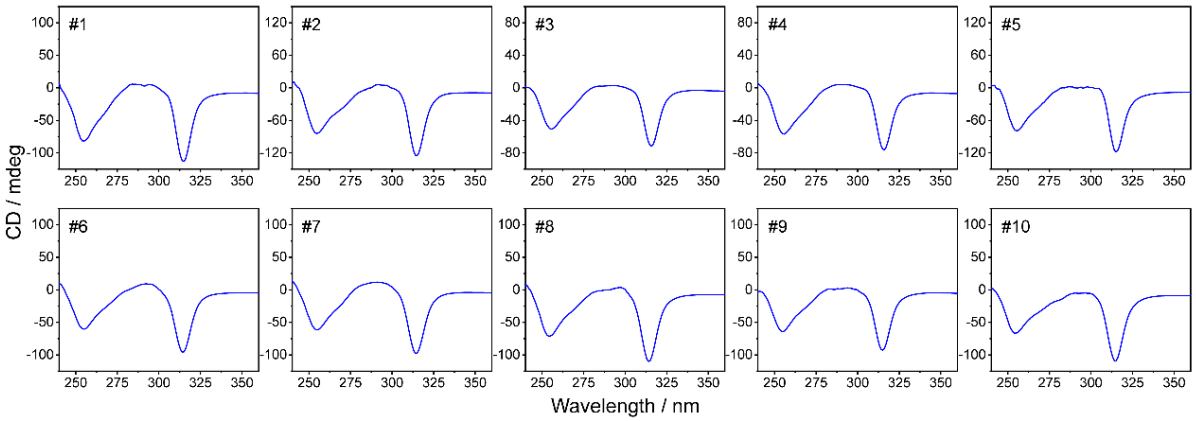

Fig. S9 Solid-state ECD spectra of 10 independent **P[5]HQ** samples crystallised in (*D*)-**EL**. Solid-phase samples were prepared using 50 mg KBr and 1 mg of crystalline powder. All 10 samples showed positive Cotton effects at 259/315 nm.

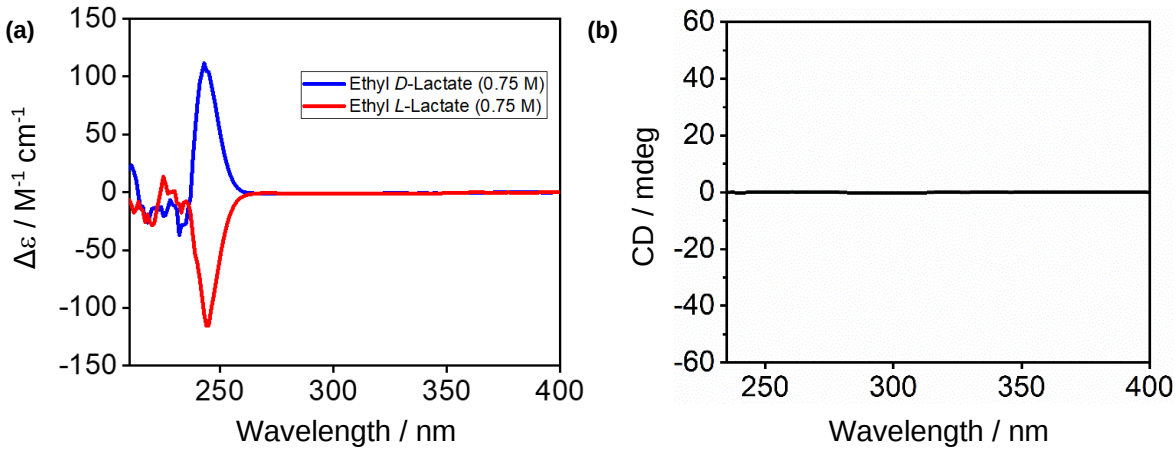

Fig. S10 (a) ECD spectra of (*L*)-**EL** (red) and (*D*)-**EL** (blue) in MeOH (0.75 M). (b) Solid-state ECD spectra of **P[5]HQ** obtained in 1:1 mixture (*L*)-**EL** and (*D*)-**EL**.

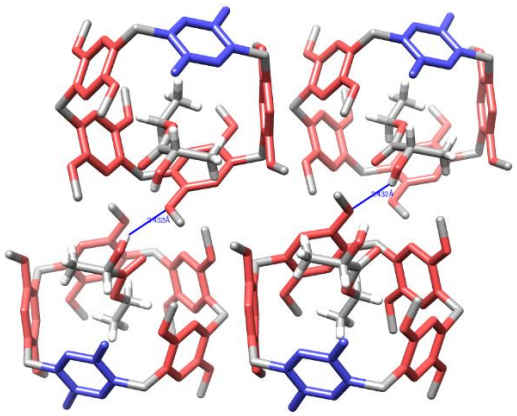

Fig. S11 Single crystal structure of [(*L*)-**EL**⊂(*M*)-**P[5]HQ**]. Intermolecular hydrogen bonding between the hydroxyl group of (*L*)-**EL** and an oxygen atom of a methoxy group on a nearby **P[5]HQ** macrocycle are highlighted (OH···O distance = 2.43 Å). Hydrogen atoms on the macrocycles are omitted for clarity.

[(*D*)-**EL**⊂(*P*)-**P[5]HQ**]: Crystalline powder of **P[5]HQ** (1.0 g) was suspended in (*D*)-**EL** (2.0 mL) in 10 mL glass vial. The mixture was heated to 100 °C until all solid completely dissolved. The mixture was then cool to room temperature slowly and left to stand for 24 h. Light red color [(*D*)-**EL**⊂(*P*)-**P[5]HQ**] crystals were collected by filtration and dried under vacuum at room temperature. ^{1}H NMR (400 MHz, $CDCl_3$) δ 7.17 (s, 2H), 6.90 (s, 2H), 6.84 (s, 2H), 6.82 (s, 2H), 6.60 (s, 2H), 6.59 (s, 2H), 4.25 (q, *J* = 6.9 Hz, 1H), 4.07 (q, *J* = 7.1 Hz, 2H), 3.83 (s, 6H), 3.80 – 3.74 (m, 12H), 3.73 (s, 6H), 3.70 – 3.65 (m, 10H), 2.77 (s, 1H), 1.41 (d, *J* = 6.9 Hz, 3H), 1.08 (t, *J* = 7.1 Hz, 3H). Similarly, [(*L*)-**EL**⊂(*M*)-**P[5]HQ**] was obtained by following the procedure described above. See Supporting Information Section 7 for X-ray crystallographic analysis.

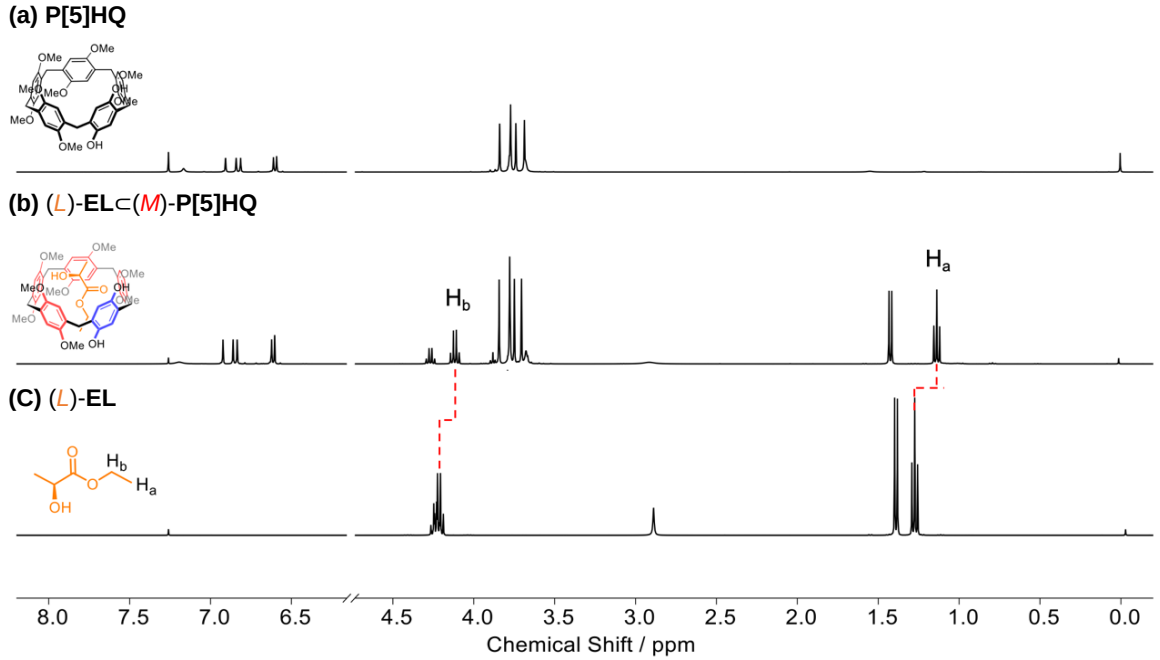

Fig. S12 ^{1} H NMR (400 MHz, $CDCl_3$) spectra of (a) **P[5]HQ**, (b) dissolved [(*L*)-**EL**⊂(*M*)-**P[5]HQ**], (c) (*L*)-**EL** recorded in $CDCl_3$ at room temperature. The proton signals of the ethyl moiety of (*L*)-**EL** showed minor upfield shift when complexed with **P[5]HQ**.

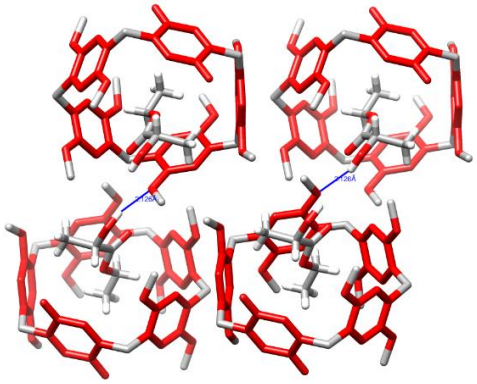

Fig. S13 Single crystal structure of [(*L*)-**EL**⊂(*M*)-**P[5]Q**]. Intermolecular hydrogen bonding between the hydroxyl group of (*L*)-**EL** and an oxygen atom of a methoxy group on a nearby **P[5]Q** macrocycle are highlighted (OH···O distance = 2.13 Å). Hydrogen atoms on the macrocycles are omitted for clarity.

- Direct crystallisation of **P[5]A** in ethyl (*L*)/(*D*)-lactate:

Crystallisation of *rac*-**P[5]A** in (*L*)-**EL**: Crystalline powder of **P[5]A** (200 mg) was suspended in (*L*)-**EL** (0.25 mL) in a 10-mL sample vial. The mixture was heated at 100 °C until all solid completely dissolved. The resulting solution was then cool to room temperature slowly and left to stand for 48 h. Colorless **P[5]A** crystals were collected by filtration and then dried under vacuum at room temperature. Crystallisation of *rac*-**P[5]A** in (*D*)-**EL** was performed in an identical manner.

- Grinding *rac*-**P[5]A** crystalline solids in aqueous solutions of *D*/*L*-ethyl lactate

Crystalline solid of *rac*-**P[5]A** (25 mg) was suspended in 5.0 M (*L*)-**EL** aqueous solution (2.0 mL) in a 2.5 mL glass sample vial. The mixture was stirred at room temperature for 24 h. The solid was then collected by filtration, washed by water (5.0 mL), and dried under vacuum at room temperature. In addition, *rac*-**P[5]**A was also ground in 5.0 M (*D*)-**EL** aqueous solution (2.0 mL) following the procedure described above.

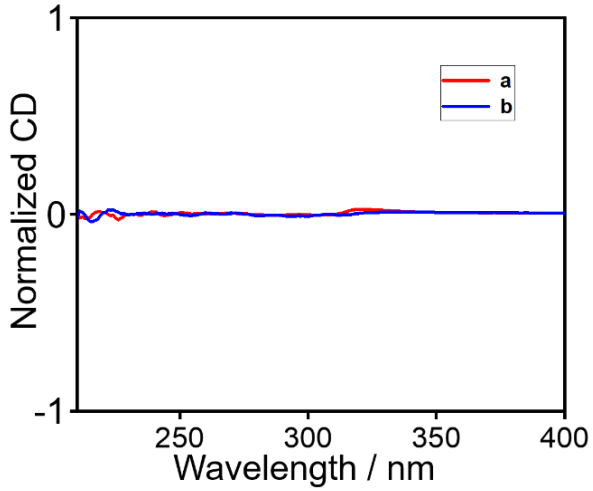

Fig. S14 Solid-state ECD spectra of **P[5]A** crystallised in (a) (*L*)-**EL** and (b) (*D*)-**EL**.

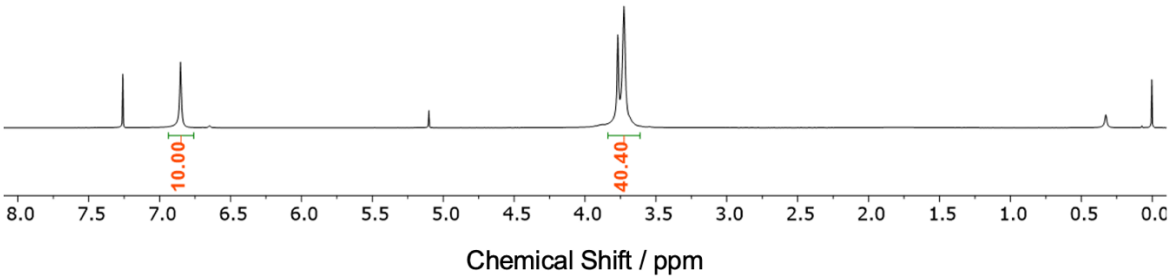

Fig. S15 ^{1}H NMR (400 MHz) spectrum of *rac*-**P[5]A** stirred in 5.0 M (*L*)-**EL** for 24 h ($CDCl_3$, 298 K).

- Stirring *rac*-**P[5]HQ** crystalline solids in aqueous solutions of *D*/*L*-ethyl lactate

rac-**P[5]HQ** (25 mg each) was suspended in 0.1, 0.5, 0.9, 1.8, 2.0, 2.2, 2.4, 2.6, 3.5, and 4.5 M (*L*)-**EL** aqueous solutions (2.0 mL each). All samples were stirred at room temperature for 24 h. The resulting crystalline solids were collected by filtration and washed with water (5.0 mL). The samples were then dried under vacuum at room temperature before being subjected to ECD analysis. The formation of [(*L*)-**EL**⊂(*M*)-**P[5]HQ**] complex is evidenced by the positive cotton effect curves shown at 315 nm in the ECD spectra. Samples stirred in (*L*)-**EL** aqueous solutions of concentrations higher than 2.6 M do not show significant difference in their relative intensities.

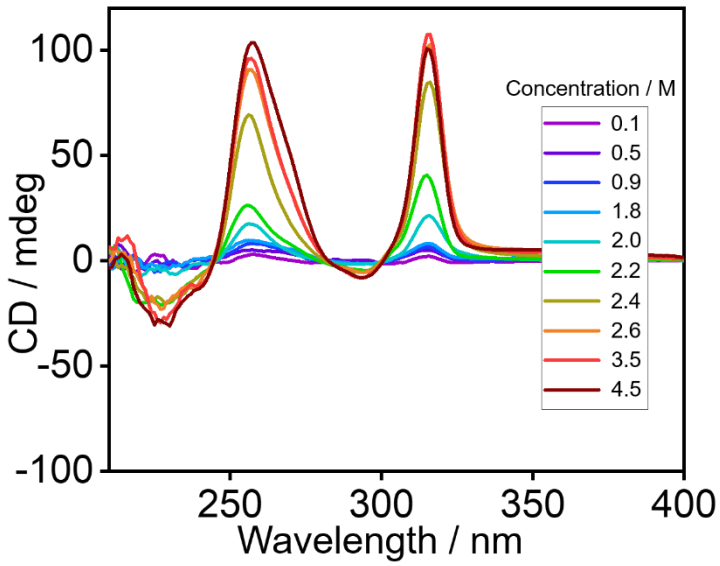

Fig. S16 Solid-state ECD spectra of **P[5]HQ** samples stirred in (*L*)-**EL** aqueous solutions ranging from 0.1 to 4.5 M for 24 h.

- Direct crystallisation of *rac*-**P[5]Q** in *D*/*L*-ethyl lactate

[(*L*)-**EL**⊂(*M*)-**P[5]Q**]: Crystalline powder of *rac*-**P[5]Q** (1.0 g) was suspended in (*L*)-**EL** (2.0 mL) in 10 mL glass vial. The mixture was heated to 100 °C until all solid completely dissolved. The mixture was then cool to room temperature slowly and left to stand for 24 h. Red color [(*L*)-**EL**⊂(*M*)-**P[5]Q**] crystals were collected by filtration and dried under vacuum at room temperature. Similarly, the [(*D*)-**EL**⊂(*P*)-**P[5]Q**] crystals can be obtained by following the procedure described above. See Supporting Information Section 7 for X-ray crystallographic analysis.

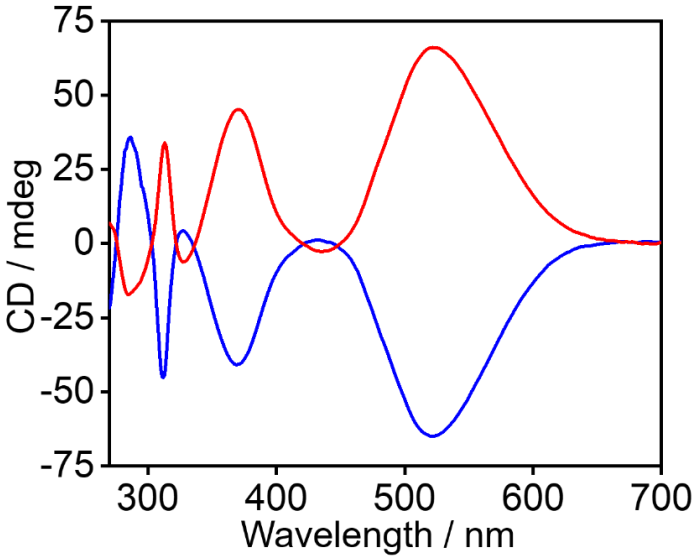

Fig. S17 Solid-state ECD spectra of [(*L*)-**EL**⊂(*M*)-**P[5]Q**] (red) and [(*D*)-**EL**⊂(*P*)-**P[5]Q**] (blue).

- Stirring *rac*-**P[5]Q** crystalline solids in aqueous solutions of *D*/*L*-ethyl lactate

rac-**P[5]Q** (25 mg each sample) was suspended in 0.5, 1.0, 1.5, 2.0, 2.5, 3.0, 3.5, 4.0, 4.5, and 5.0 M (*L*)-**EL** aqueous solutions (2.0 mL each). All samples were stirred at room temperature for 24 h. The resulting crystalline solids were collected by filtration and washed with water (5.0 mL). The samples were then dried under vacuum at room temperature before being subjected to ECD analysis. The formation of [(*L*)-**EL**⊂(*M*)-**P[5]Q**] complex is evidenced by the positive cotton effect curves shown at 312, 370, and 520 nm in the ECD spectra. Samples stirred in (*L*)-**EL** aqueous solutions with concentrations higher than 4.0 M do not show significant difference in their relative intensities.

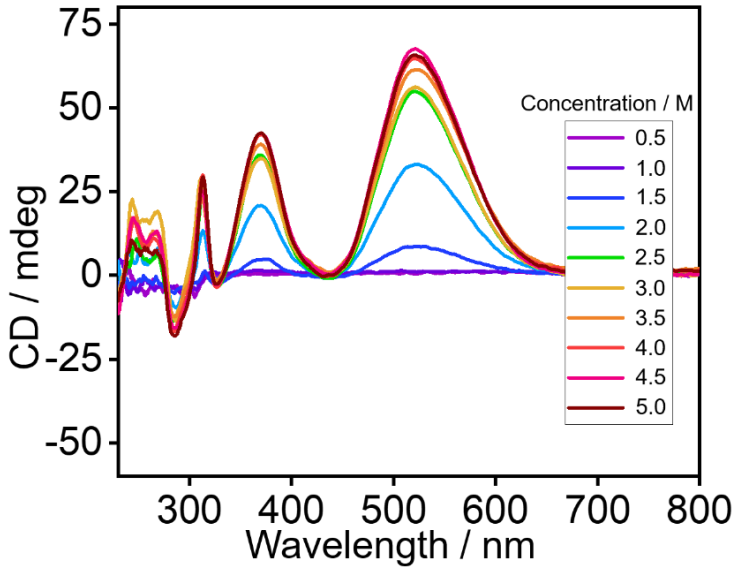

Fig. S18 Solid-state ECD spectra of **P[5]Q** samples stirred in (*L*)-**EL** aqueous solutions ranging from 0.5 to 5.0 M for 24 h.

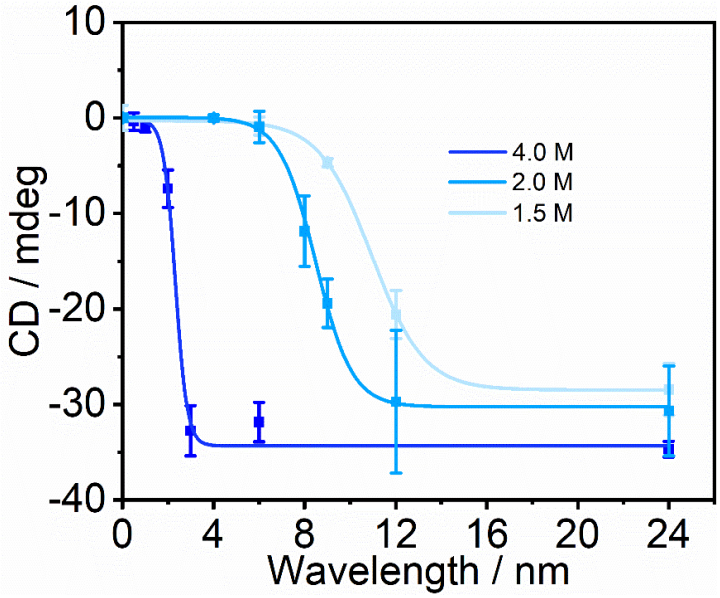

Fig. S19 Evolution of CD intensity at 520 nm for **P[5]Q** samples stirred in 4.0, 2.0 and 1.5 M (*D*)-**EL** aqueous solutions.

- Stability of [(*D*)-**EL**⊂(*P*)-**P[5]HQ**] complex

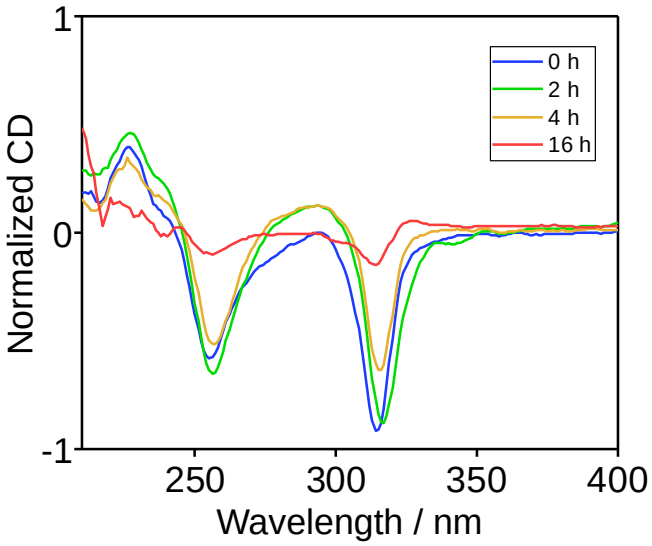

Fig. S20 Solid-state ECD spectra of [(*D*)-**EL**⊂(*P*)-**P[5]HQ**] crystalline powder after being mechanically-ground for different time intervals. Crystalline powders of [(*D*)-**EL**⊂(*P*)-**P[5]HQ**] complex (100 mg) was subjected to mechanical balling (with a 15 min halt every 2 h to avoid overheating). Samples were collected after 0, 2, 4, and 16 h of mechanical grinding for ECD analysis. The [(*D*)-**EL**⊂(*P*)-**P[5]HQ**] sample underwent gradual racemisation over the ball-milling process.

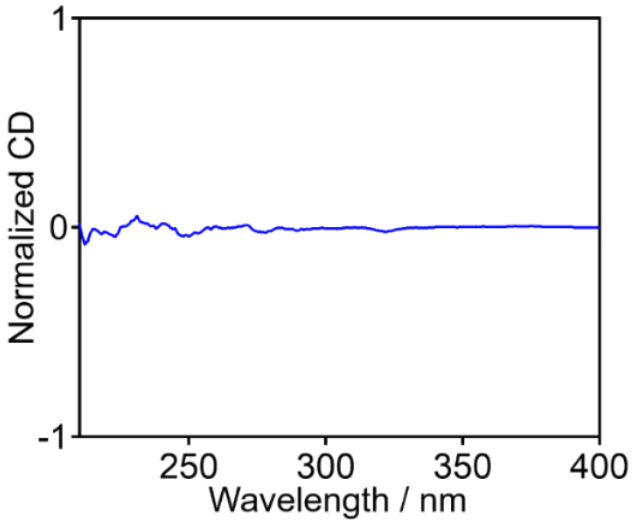

Fig. S21 Solid-state ECD spectra of [(*D*)-**EL**⊂(*P*)-**P[5]HQ**] sample after being heated at 110 °C under high vacuum for 24 h. No obvious Cotton effect was observed.

7. X-Ray Crystallography

Single crystals suitable for X-ray diffraction were selected and mounted in inert oil in cold gas stream and their X-ray diffraction intensity data was collected on a Rigaku XtaLAB FRX diffractometer equipped with a Hypix6000HE detector, using Cu $K\alpha$ radiation (λ = 1.54184 Å). Crystals were kept at the temperature listed in **Table S1-S2** during data collection. By the use of Olex2,[11] The structures were solved by intrinsic phasing methods and refined by full-matrix least squares using the SHELX-TL package.[12] The hydrogen atoms were set in calculated positions and refined as riding atoms with a common fixed isotropic thermal parameter. Selected details of the data collection and structural refinement of each compound can be found within **Table S1-S2** and full details are available in the corresponding CIF files. Crystallographic data (excluding structure factors) have been deposited with the Cambridge Crystallographic Data Centre and may be obtained free of charge via http://www.ccdc.cam.ac.uk/data_request/cif. Powder X-ray diffraction (PXRD) patterns were recorded on a Rigaku D/Max-2500 X-ray diffractometer. Data were collected over the range of 3−40° at a scan rate of 5°·min^{-1}.

Table S1. Crystal data and structure refinement for [(*L*)-**EL**⊂(*M*)-**P[5]HQ**]

Empirical formula	$C_{48}H_{56}O_{13}$
Formula weight / g mol^{-1}	840.93
Temperature / K	200.00(10)
Crystal system	monoclinic
Space group	*C*2
a / Å	21.2498(2)
b / Å	11.99340(10)
c / Å	17.88350(10)
α / °	90
β / °	98.7260(10)
γ / °	90
Volume/ Å^3	4504.99(6)
Z	4
ρ_{calc} / g cm^{-3}	1.240
μ / mm^{-1}	0.737
F / 000	1792.0
2θ range for data collection / °	5.00 to 149.168
Crystal size / mm^3	0.2 × 0.1 × 0.1
Index ranges	$-24 \leq h \leq 26$, $-14 \leq k \leq 14$, $-22 \leq l \leq 22$
Reflections collected	42011
Independent reflections	8931 [R_{int} = 0.0275, R_{sigma} = 0.0179]
Data/restraints/parameters	8931/1/563
Goodness-of-fit on F^2	1.031
Final *R* indices [I >2σ(I)]	R = 0.0401, wR_2 = 0.1126
Final *R* indices [all data]	R_1 = 0.0416, wR_2 = 0.1146
Largest diff. peak / hole / e Å^3	0.33/-0.25
CCDC No.	2073656
Crystallisation solvents	ethyl *L*-lactate

Table S2. Crystal data and structure refinement for [(*L*)-**EL**⊂(*M*)-**P[5]Q**]

Empirical formula	$C_{48}H_{54}O_{13}$
Formula weight / g mol^{-1}	838.91
Temperature / K	159.99(10)
Crystal system	monoclinic
Space group	*C*2
a / Å	21.1145(4)
b / Å	12.0659(3)
c / Å	17.7473(3)
α / °	90
β / °	98.805(2)
γ / °	90
Volume/ Å^3	4468.11(16)
Z	4
ρ_{calc} / g cm^{-3}	1.247
μ / mm^{-1}	0.743
F / 000	1784.0
2θ range for data collection / °	5.038 to 154.92
Crystal size / mm^3	0.02 × 0.01 × 0.01
Index ranges	$-26 \leq h \leq 26$, $-14 \leq k \leq 13$, $-22 \leq l \leq 21$
Reflections collected	41754
Independent reflections	8631 [R_{int} = 0.0610, R_{sigma} = 0.0439]
Data/restraints/parameters	8631/3/568
Goodness-of-fit on F^2	1.036
Final *R* indices [I >2σ(I)]	R_1 = 0.0509, wR_2 = 0.1228
Final *R* indices [all data]	R_1 = 0.0710, wR_2 = 0.1375
Largest diff. peak / hole / e Å^3	0.37/-0.30
CCDC No.	2073655
Crystallisation solvents	ethyl *L*-lactate

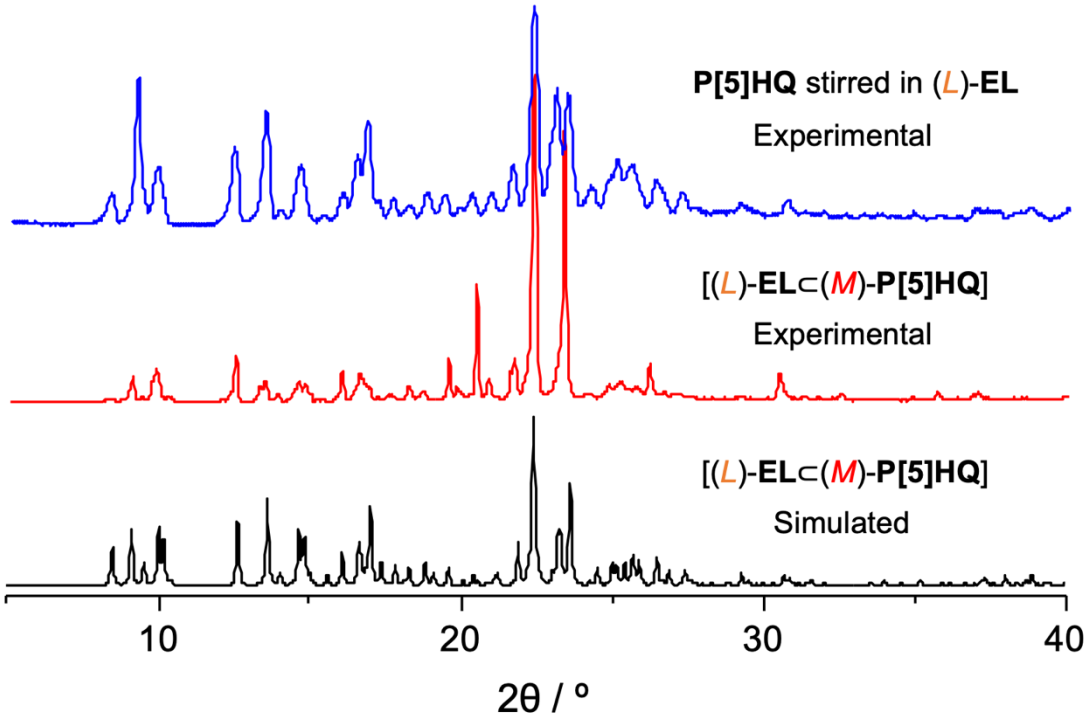

Fig. S22 Powder X-ray diffraction (PXRD) patterns of (bottom to top) simulated **P[5]HQ**, [(*L*)-**EL**⊂(*M*)-**P[5]HQ**] complex (by crystallisation), and [(*L*)-**EL**⊂(*M*)-**P[5]HQ**] complex (by partly soluble state).

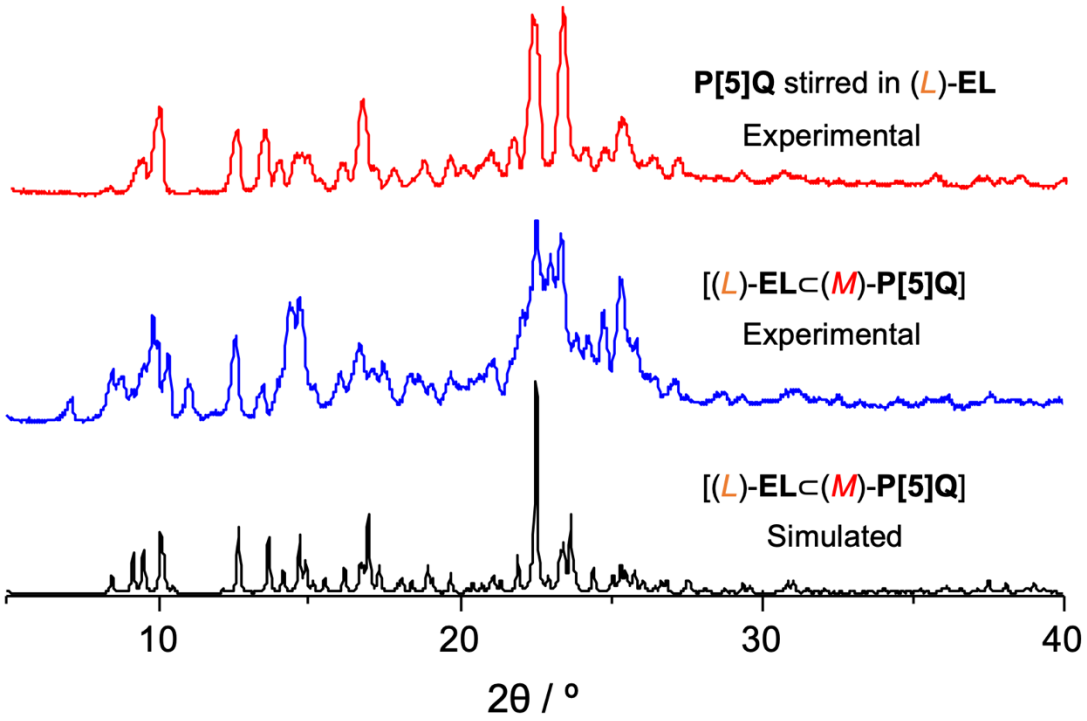

Fig. S23 Powder X-ray diffraction (PXRD) patterns of (bottom to top) simulated **P[5]Q**, [(*L*)-**EL**⊂(*M*)-**P[5]Q**] complex (by crystallisation), and [(*L*)-**EL**⊂(*M*)-**P[5]Q**] complex (by partly soluble state).

8. References

1. T. Boinski and A. Szumna, *Tetrahedron*, 2012, **68**, 9419–9422.
2. C. Han, Z. Zhang, G. Yu and F. Huang, *Chem. Commun*., 2012, **48**, 9876–9878.
3. S. Grimme, *J. Comput. Chem.*, 2006, **27**, 1787–1799.
4. F. Weigend and R. Ahlrichs, *Phys.Chem.Chem.Phys.*, 2005, **7**, 3297–3305.
5. J.-D. Chai and M. Head-Gordon, *Phys. Chem. Chem. Phys.*, 2008, **10**, 6615–6620.
6. N. Harada, S. L. Chen and K. Nakanishi, *J. Am. Chem. Soc.*, 1975, **97**, 5345–5352.
7. A. Klamt and G. Schüürmann, *J. Chem. Soc. Perkin Trans.*, 1993, **2**, 799–805.
8. K. K. Baldridge, A. Klamt, *J. Chem. Phys.*, 1997, **106**, 6622–6633.
9. M. D. Hanwell, D. E. Curtis, D. C. Lonie, T. Vandermeersch, E. Zurek, G. R. Hutchison, *J. Cheminform.*, 2012, **4**, 17.
10. Gaussian 16, Revision C.01, M. J. Frisch, G. W. Trucks, H. B. Schlegel, G. E. Scuseria, M. A. Robb, J. R. Cheeseman, G. Scalmani, V. Barone, G. A. Petersson, H. Nakatsuji, X. Li, M. Caricato, A. V. Marenich, J. Bloino, B. G. Janesko, R. Gomperts, B. Mennucci, H. P. Hratchian, J. V. Ortiz, A. F. Izmaylov, J. L. Sonnenberg, D. Williams-Young, F. Ding, F. Lipparini, F. Egidi, J. Goings, B. Peng, A. Petrone, T. Henderson, D. Ranasinghe, V. G. Zakrzewski, J. Gao, N. Rega, G. Zheng, W. Liang, M. Hada, M. Ehara, K. Toyota, R. Fukuda, J. Hasegawa, M. Ishida, T. Nakajima, Y. Honda, O. Kitao, H. Nakai, T. Vreven, K. Throssell, J. A. Montgomery, Jr., J. E. Peralta, F. Ogliaro, M. J. Bearpark, J. J. Heyd, E. N. Brothers, K. N. Kudin, V. N. Staroverov, T. A. Keith, R. Kobayashi, J. Normand, K. Raghavachari, A. P. Rendell, J. C. Burant, S. S. Iyengar, J. Tomasi, M. Cossi, J. M. Millam, M. Klene, C. Adamo, R. Cammi, J. W. Ochterski, R. L. Martin, K. Morokuma, O. Farkas, J. B. Foresman, and D. J. Fox, Gaussian, Inc., Wallingford CT, 2016.
11. O. V. Dolomanov, L. J. Bourhis, R. J. Gildea, J. A. K. Howarda and H. Puschmann, *J, Appl. Cryst*., 2009, **42**, 339–341.
12. G. M. Sheldrick, *Acta Cryst. Sect*., 2008, **64**, 112–122.